Secondary structure of the IIB domain of the *Escherichia coli* mannose transporter, a new fold in the class of α/β twisted open-sheet structures

Ruth M. Gschwind[a], Gerd Gemmecker[a,*], Michael Leutner[a], Horst Kessler[a], Regula Gutknecht[b], Regina Lanz[b], Karin Flükiger[b], Bernhard Erni[b]

[a]*Institut für Organische Chemie und Biochemie II, Technische Universität München, D-85747 Garching, Germany*
[b]*Department für Chemie und Biochemie, Universität Bern, CH-3012 Bern, Switzerland*

Received 25 November 1996

Abstract The mannose transporter of the *Escherichia coli* bacterial phosphotransferase system consists of three subunits: IIAB, IIC and IID. $IIAB^{Man}$ transfers phosphoryl groups to the transported substrate via phosphohistidine intermediates. Its IIB domain was overexpressed and isotopically labelled with ^{13}C, ^{15}N and ^{2}H. Heteronuclear 3D triple-resonance NMR experiments combined with a semi-automatic assignment procedure yielded the sequential assignment of the ^{1}H, ^{13}C and ^{15}N backbone resonances. Based on the evaluation of conformationally sensitive parameters, the secondary structure of the IIB^{Man} domain has been determined as an α/β twisted open-sheet structure consisting of a six-stranded parallel β-sheet with the novel strand order 3–2–4–1–5–6, six helices and a short two-stranded antiparallel β-sheet.

Key words: Bacterial phosphotransferase system; Heteronuclear NMR; Secondary structure; Histidine phosphate; (*Escherichia coli*)

1. Introduction

The bacterial phosphoenolpyruvate-dependent phosphotransferase system (PTS) consists of a protein phosphorylation cascade which integrates transport and metabolism of carbohydrates with signal transduction [2,3]. It is almost ubiquitous in bacteria but does not occur in animals and higher plants. The mannose PTS transporter of *Escherichia coli* mediates the uptake of mannose and related hexoses by a mechanism coupling vectorial translocation and concomitant phosphorylation of the substrate. It consists of two transmembrane subunits (IIC^{Man} and IID^{Man}) and a soluble hydrophilic subunit ($IIAB^{Man}$) [4]. Compared to other PTS transporters it shows a wide substrate specificity, an unusual subunit composition and a different molecular reaction mechanism [5]. The IIAB subunit consists of two independently folding domains, IIA mediating interdimer contacts and IIB binding to the transmembrane IIC/IID complex. Phosphoryl transfer from HPr to the transported sugar substrate occurs sequentially via the phosphorylation sites of IIA and IIB (His^{10} and His^{175}, respectively) [6]. Phospho-HPr itself is regenerated from phosphoenolpyruvate in a reaction catalysed by Enzyme I of the PTS.

Uniqueness and pleiotropic function make the PTS a potential target for the development of new antimicrobials. A desirable prerequisite for this enterprise is structural information about its components. The 3D structures of a number of PTS proteins are already known (for a review see [7]). Here we present the secondary structure of the IIB^{Man} domain obtained by heteronuclear NMR spectroscopy. IIB^{Man} consists of a central six-stranded parallel β-sheet with the novel strand order 3–2–4–1–5–6 and six α-helices. Assuming that the alternating α and β structures form right-handed turns, IIB^{Man} must have an open-pleated-sheet structure with helices 1 and 2 on one and helices 3, 4 and 5 on the opposite side of the β-sheet.

2. Materials and methods

2.1. Overexpression and purification of IIB^{Man}

The expression plasmid pMSP20 encoding the IIB^{Man} domain was constructed by inserting the *NdeI*/*ScaI* fragment of pTSL23 [4] into the expression vector pMS470 encoding Ptac, a ribosome-binding site, lacIq and bla (gift of Dr. E. Lanka, Berlin). *E. coli* strain W3110 (pMSP20) was grown as described [8] in a minimal salts medium supplemented with 1 g/l U-[^{15}N]NH_4Cl and either 1% glycerol or 0.25% U-[^{13}C]glucose (Martek Corp.). For the partially deuterated ^{15}N,^{13}C-labelled sample cells were grown in a minimal salts medium containing 75% D_2O and a [U-^{15}N,^{13}C, 75% D]-labelled hydrolysate from algae as amino acid source (EMBL labelling facility, EMBL, Heidelberg, Germany). The average yield after purification [4,8] was ca. 15 mg IIB^{Man} per liter of cell culture. Subclonal IIB^{Man} comprises 168 residues, with its first residue Met^{1} and the active site His^{20} corresponding to Met^{156} and His^{175} of the full-length $IIAB^{Man}$ protein.

2.2. NMR spectroscopy

All NMR experiments were performed at 300 K on four channel Bruker AMX600, DMX600 or DMX750 spectrometers, all equipped with pulsed field gradient (PFG) accessory and triple or quadruple resonance probes. Proton chemical shifts were referenced to external TSP (300 K, pH 7.0), nitrogen and carbon chemical shifts in terms of the frequency ratios Ξ according to Wishart et al. [9]. Carrier positions were 119 (^{15}N), 175 (^{13}CO), 54 ($^{13}C^{\alpha}$), 45 ($^{13}C^{\alpha/\beta}$) and 4.74 ppm (^{1}H). In all amide proton detected 2D and 3D experiments PFGs were used for coherence pathway selection with sensitivity enhancement [10,11] in the echo/antiecho manner [12] and for suppression of the water signal and spectral artifacts [13]. Quadrature detection in the other indirect dimension was achieved with the States-TPPI method [14].

All NMR spectra were acquired in 90% H_2O/10% D_2O at 600 MHz (except where stated), for general references see review [1]. The following 3D triple resonance experiments were performed with the uniformly $^{13}C/^{15}N$-labelled sample (0.9 mmol), with the ^{15}N dimensions recorded in a constant time manner [15,16]: HNCO with water flip back [17]; HCACO; HN(CA)HA; HNCACB (750 MHz); HN(CO)-

*Corresponding author. Fax (49) 89-289-13210.
E-mail: gg@artus.org.chemie.tu-muenchen.de

Abbreviations: PTS, phosphoenolpyruvate-dependent carbohydrate phosphotransferase system; $IIAB^{Man}$, hydrophilic subunit of the mannose transporter (EC 2.7.1.69); IIC^{Man} and IID^{Man}, transmembrane subunits of the mannose transporter (EC 2.7.1.69); IIB^{Man}, carboxy terminal domain of $IIAB^{Man}$; HPr, histidine-containing phosphocarrier protein of the PTS; NMR-specific abbreviations (2D, 3D, NOESY, TOCSY, etc.) see review [1]

PII S0014-5793(97)00084-7

Table 1
Backbone ^{15}N, ^{1}H and ^{13}C chemical shifts for IIB^{Man}

Residue	^{15}N	HN	CO	H^{α}	C^{α}	C^{β}	Others
Met[1]			174,0		55,7	32,9	
Gly[2]	113,6	9,24			44,7		
Pro[3]			178,2	4,43	64,8	32,1	
Asn[4]	115,7	8,63	175,3	4,93	53,5	38,5	N^{d} 113,0; H^{δ} 6,95;7,61
Asp[5]	119,7	7,89	173,0	4,58	55,2	42,0	
Tyr[6]	115,5	7,09	177,1	4,62	57,2	44,3	
Met[7]	122,0	8,95	173,7	4,58	56,8	33,3	
Val[8]	123,7	9,22	175,2	4,07	61,8	33,7	
Ile[9]	127,7	8,99	176,1	4,29	59,9	35,2	
Gly[10]	119,4	9,66	173,0	3,23	45,9		
				4,07			
Leu[11]	117,6	7,34	173,0	4,36	55,1	46,2	
Ala[12]	103,3	9,21	173,8	5,33	50,4	19,4	
Arg[13]	124,8	9,25	175,1	5,92	52,8	33,4	
Ile[14]	126,1	9,13	175,4	4,47	60,0	39,2	
Asp[15]	129,8	9,19	176,4	5,39	53,6	41,4	
Asp[16]	125,2	8,51	177,3	4,15	55,6	39,1	
Arg[17]	114,1	7,52	176,6	4,30	56,4	29,8	
Leu[18]	116,4	8,41	174,5	3,65	56,9	40,1	
Ile[19]	119,6	6,61		3,74	62,1		
His[20]	122,3	7,15			54,0	31,8	
Gly[21]							
Gln[22]	109,1	6,85	179,6	3,94	59,4	30,0	
Val[23]	119,9	8,24	177,4	3,61	65,7	31,6	
Ala[24]	118,0	7,58	179,1	4,16	54,9	18,8	
Thr[25]	111,4	7,92	175,5	4,02	63,9	69,0	
Arg[26]	121,5	8,07	178,4	4,18	59,6	30,3	
Trp[27]	116,6	8,28	179,6	4,36	61,7	29,8	N^{ε} 127,8; H^{ε} 9,97
Thr[28]	114,7	7,93	176,1	4,26	66,3	68,0	
Lys[29]	121,7	7,53	180,1	4,19	58,7	32,4	
Glu[30]	118,0	8,38	178,3	4,04	58,7	29,9	
Thr[31]	106,4	7,61	174,8	4,46	62,4	69,6	
Asn[32]	120,5	7,84	175,0	4,52	54,0	37,2	
Val[33]	110,8	7,32	175,4	4,61	60,1	33,9	
Ser[34]	112,8	8,93	174,6	4,86	58,3	64,5	N^{d} 111,0; H^{δ} 6,81;7,58
Arg[35]	120,7	7,49	174,7	5,46	55,1	35,4	
Ile[36]	124,4	9,07	174,6	4,84	60,5	41,8	
Ile[37]	126,9	9,29	175,2	4,67	60,1	39,3	
Val[38]	128,6	9,17	173,7	4,22	61,6	32,4	
Val[39]	129,9	8,63	175,1	4,48	60,1	30,8	
Ser[40]	118,6	8,54	174,2	4,4	57,7	64,0	
Asp[41]	104,5	9,84		3,8	57,5		
Glu[42]	122,1	8,02	178,4	4,07	57,2		
Val[43]	120,8	7,78	174,4	4,13	66,4	32,4	
Ala[44]	120,5	7,92	178,0	3,7	54,9	18,9	
Ala[45]	116,9	6,94	176,7	4,32	52,0	19,2	
Asp[46]	121,1	7,56	175,0	4,37	52,1	41,5	
Thr[47]	119,1	8,28	176,7	3,75	66,2	68,6	
Val[48]	123,0	8,14	178,3	3,75	66,2	31,9	
Arg[49]	121,2	7,75	178,9	3,91	59,2	31,2	
Lys[50]	118,1	8,76	178,3	3,81	60,5	31,9	
Thr[51]	116,1	7,78	176,4	3,98	66,2	68,8	
Leu[52]	122,7	7,75	179,7	4,06	58,0	41,8	
Leu[53]	118,2	8,04	177,9	4,04	57,5	42,3	
Thr[54]	106,8	7,49	176,7	3,96	64,4	69,1	
Gln[55]	119,4	7,62	177,3	4,31	57,3	29,2	N^{ε} 110,9; H^{ε} 6,80;7,39
Val[56]	113,2	7,35	174,9	4,39	61,0	31,7	
Ala[57]	124,9	7,23	174,4	4,15	50,7	17,9	
Pro[58]				3,9			
Pro[59]			178,3		63,6	31,3	
Gly[60]	111,7	8,72	173,8	4,31	45,4		
				4,17			
Val[61]	120,6	7,83	173,3	4,52	60,2	34,1	
Thr[62]	117,4	7,74	172,7	4,44	61,2	69,7	
Ala[63]	125,8	8,49	175,6	5,67	49,8	22,1	
His[64]	118,6	8,53	173,6	4,78	54,1	33,6	
Val[65]	122,5	8,88	175,0	5,02	60,9	33,8	
Val[66]	120,6	9,23	172,8	4,78	58,5	36,2	
Asp[67]	118,4	7,64	175,1	4,39	52,0	41,3	
Val[68]	120,0	8,54	177,3	3,55	67,8	31,6	
Ala[69]	120,0	8,54	181,5	3,93	55,4	17,9	

Table 1 (*continued*).

Residue	^{15}N	HN	CO	H^{α}	C^{α}	C^{β}	Others
Lys[70]	121,1	8,46	178,2	3,97	59,0	32,4	
Met[71]	119,4	8,38	177,8	4,48	56,6	31,2	
Ile[72]	119,4	7,74	178,0	3,37	66,1	38,1	
Arg[73]	118,8	7,31	180,3	4,19	60,0	30,3	
Val[74]	122,3	8,92	177,5	3,8	66,1	31,9	
Tyr[75]	118,8	8,67	176,2	4,22	60,9	39,5	
Asn[76]	112,7	7,28	173,0	4,6	53,6	40,2	
Asn[77]	121,0	7,79		5,09	50,5	40,2	
Pro[78]			177,8	4,45	64,1		
Lys[79]	121,8	8,19	177,1	3,84	58,7	32,1	
Tyr[80]	116,2	7,00	174,4	4,55	56,3	38,2	
Ala[81]	121,5	7,13	179,5	3,32	54,0	19,0	
Gly[82]	110,9	7,80	174,1	4,24	45,9		
				3,67			
Glu[83]	122,5	8,11	175,7	4,2	57,2	30,5	
Arg[84]	123,8	9,05	176,4	5,16	55,8	32,1	
Val[85]	115,9	9,35	175,2	5,17	59,2		
Met[86]	124,9	8,76	174,0	5,24	53,3	36,6	
Leu[87]	126,5	9,05	175,0	5,28	52,7	44,4	
Leu[88]	123,5	8,59	173,8	5,50	52,5	47,2	
Phe[89]	117,1	8,74	176,0	5,04	54,5	44,1	
Thr[90]	109,0	10,48	173,7	4,41	61,9	69,8	
Asn[91]	114,8	7,55		4,78	52,3	40,8	
Pro[92]			177,4	3,98	63,4	34,1	
Thr[93]	124,9	8,03	177,3	3,64	68,5	67,3	
Asp[94]	122,0	8,33	177,0	4,37	57,5	40,6	
Val[95]	118,2	6,43	177,3	2,84	65,4	30,1	
Glu[96]	121,2	7,29	178,0	4,14	58,8	27,4	
Arg[97]	117,8	8,27	179,7	3,95	59,2	31,9	
Leu[98]	120,3	7,64	179,0	3,85	57,7	41,6	
Val[99]	120,7	8,31	181,7	4,01	65,6	31,6	
Glu[100]	124,8	8,86	178,1	3,96	59,0	28,9	
Gly[101]	104,6	7,49	174,0	4,24	45,1		
				3,50			
Gly[102]	106,8	7,74	174,3	4,39	45,0		
				3,61			
Val[103]	121,9	7,64	176,1	3,05	62,7	30,6	
Lys[104]	128,3	6,23	174,4	4,19	56,4	31,0	
Ile[105]	127,2	7,28	175,4	4,18	60,6	40,4	
Thr[106]	115,7	8,67	175,4	4,47	62,4	69,5	
Ser[107]	118,7	7,67	173,3	5,1	57,4	63,2	
Val[108]	131,4	9,51		4,57	60,8	35,1	
Asn[109]	126,8	9,07	177,0	5,21	52,2	42,3	
Val[110]	129,8	10,21	174,2	3,96	62,9	31,0	
Gly[111]	116,8	9,09	175,7	3,32	46,1		
				4,39			
Gly[112]	109,9	8,05	171,9	4,29	47,7		
				3,99			
Met[113]	126,0	8,67	175,2	4,61	55,7	37,7	
Ala[114]	129,9	10,43	177,9	4,13	53,2	19,8	
Phe[115]	121,4	8,60	175,5	3,89	60,9	39,1	
Arg[116]	123,1	5,73	173,3	4,01	53,9	33,2	
Gln[117]	120,1	8,42	179,0	3,84	58,1	28,1	N^{ε} 112,7; H^{ε} 6,98;7,66
Gly[118]	115,0	8,94	175,1	4,48	44,7		
				3,70			
Lys[119]	118,4	7,89	175,0	4,51	56,2	35,3	
Thr[120]	117,0	9,19	174,2	4,61	62,4	70,5	
Gln[121]	129,5	9,37	176,3	4,87	57,2	29,0	N^{ε} 110,8; H^{ε} 6,63;6,97
Val[122]	122,3	8,84	175,7	4,42	62,5	32,1	
Asn[123]	119,1	8,46	178,7	4,55	55,9	39,1	N^{d} 109,6; H^{δ} 6,78;7,57
Asn[124]	119,6	8,16	175,3	4,27	56,8	39,4	
Ala[125]	118,9	7,97	177,3	4,57	52,1	21,3	
Val[126]	120,6	7,83	175,1	4,47	63,0	35,1	
Ser[127]	125,3	8,26	172,8	5,57	58,4	66,1	
Val[128]	111,1	8,79	175,6	5,61	58,3	37,0	
Asp[129]	123,1	9,17	173,6	5,22	51,7	43,4	
Glu[130]	116,9	8,81	178,9	3,98	60,4	29,2	
Lys[131]	122,3	7,82	179,9	4,09	59,0	31,6	
Asp[132]	121,1	8,47	179,6	4,05	57,3	41,8	
Ile[133]	119,1	8,49	177,3	3,58	67,0	38,2	
Glu[134]	119,8	8,15	179,4	4,02	59,4	29,8	
Ala[135]	121,4	7,61	179,9	3,99	55,5	18,0	

Table 1 (*continued*).

Residue	^{15}N	HN	CO	H^{α}	C^{α}	C^{β}	Others
Phe[136]	116,2	8,58	175,3	4,33	62,1	37,6	
Lys[137]	119,1	8,93	180,4	3,89	60,9	32,3	
Lys[138]	122,2	8,03	180,0	3,97	60,1	32,5	
Leu[139]	120,7	8,32	179,4	3,94	58,3	42,8	
Asn[140]	118,4	9,03	179,2	4,38	57,3	40,2	
Ala[141]	122,9	8,25	179,1	4,16	54,5	18,0	
Arg[142]	115,9	7,28	177,1	4,31	56,7	31,5	
Gly[143]	107,8	8,18	174,6	3,82 4,14	45,2		
Ile[144]	122,6	7,05	175,5	3,68	61,2	38,9	
Glu[145]	130,0	7,75	174,6	4,17	56,9	30,2	
Leu[146]	128,5	8,55	174,9	5,12	53,0	45,0	
Glu[147]	123,9	9,03	173,8	5,46	52,7	30,8	
Val[148]	124,4	9,21	176,7	4,53	60,9	33,3	
Arg[149]	123,1	7,01	176,6	4,66	57,1	37,7	
Lys[150]	127,6	9,50	178,5	4,36	61,1	32,8	
Val[151]	112,7	8,08	177,9	4,56	59,7	35,3	
Ser[152]	118,0	8,09	175,2		61,6		
Thr[153]	107,7	6,70	175,4	4,08	61,0	68,3	
Asp[154]	125,8	7,56		4,7	53,6	40,2	
Pro[155]			181,6	4,34	62,5	31,7	
Lys[156]	122,1	8,50	177,2	4,13	57,6	33,4	
Leu[157]	125,6	7,78	178,4	4,72	53,5	43,7	
Lys[158]	122,3	9,01	177,9	4,66	55,8	31,6	
Met[159]	125,7	8,06	178,2	4,04	57,2	33,8	
Met[160]	113,5	9,35	179,9	4,37	56,0	28,2	
Asp[161]	120,1	7,05	178,3	4,5	57,0	40,0	
Leu[162]	119,5	7,36	179,7	4,12	57,2	41,1	
Ile[163]	115,4	7,79	177,6	3,83	63,9	38,2	
Ser[164]	116,4	7,85	175,2	4,29	60,9	62,9	
Lys[165]	119,0	7,34	174,4	4,27	57,0	32,7	
Ile[166]	117,0	7,44	175,8	4,15	62,1	38,7	
Asn[167]	124,4	8,08	174,8	4,62	54,4	41,3	
Lys[168]	126,6	7,73	175,7	4,19	57,3	34,0	

CACB [18] (750 MHz); ^{13}C-NOESY-HSQC (750 MHz). The following spectra were obtained from the ^{15}N-labelled sample: ^{15}N-NOESY-HSQC (τ_m=100 ms); ^{15}N-TOCSY-HSQC (τ_m=19 ms, with a DIPSI-2 mixing sequence [19]). In addition two ^{15}N-NOESY-HSQC-spectra and a HNHA-spectrum [20] were recorded on the 75% deuterated $^{13}C/^{15}N$-labelled sample (with ^{2}H-decoupling using GARP [21]). The data were processed with the software packages UXNMR (Bruker) and NMR-TRIAD (Tripos). For the indirect dimensions linear prediction, zero filling (to next power of 2) and apodization with a 90° shifted sine bell were used, in the direct dimension zero filling to 1024 real points, Lorentz-to-Gauss transformation and baseline correction were applied.

3. Results and discussion

3.1. Resonance assignment

For a 20 kDa protein, IIB^{Man} exhibited a comparatively poor signal intensity in most of its 3D spectra, and the ^{1}H and ^{13}C signals in particular decayed rapidly. The residues around the active site His^{20} and in the whole amino-terminal half of the protein displayed low signal intensities, or no signals at all. Many amide resonances in this region even showed almost no NOE cross-peaks. In addition, a large percentage of the expected signals was missing in the NMR experiments containing long periods for coupling evolution. Nevertheless, the degeneracy of the resonances and the low information content could be overcome by combining the sequence information from C^{α}, C^{β}, CO and H^{α} signals, and an almost complete proton, carbon and nitrogen assignment of the IIB^{Man} backbone was obtained (Table 1). The sequential backbone assignment was performed with the program PASTA (Protein Assignment by Threshold Accepting) [22], using a minimization strategy termed *threshold accepting*, similar to simulated annealing. PASTA uses peaklists from the HNCO spectrum to create a basis set of pseudo-residues. Information from the HNCO, HNCA, HN(CA)HA, HCACO, HNCACB, HN(CO)CACB, TOCSY and HNHA spectra was then combined to achieve the sequential assignment. For this the program utilizes a penalty function defined on the basis of the match between two adjacent residues. This penalty function is then minimized to find the sequence with the lowest 'energy', representing the assignment that matches the current dataset best.

3.2. Secondary structure of IIB^{Man}

Secondary structure elements were characterized by a specific pattern of sequential and long-range NOE cross-peaks [23]. However, the number of cross-peaks obtained from the $^{15}N/^{13}C$- and the ^{15}N-labelled sample was too low for unambiguous secondary structure determination. Only a new 75% deuterated $^{13}C/^{15}N$-labelled sample afforded significantly improved signal intensities (cf., Fig. 1) [24]. However, the overall number and the intensities of NOE cross-peaks from the amino-terminal half still remained considerably lower than from the carboxy-terminal moiety of IIB. Interresidual NOE data for each residue in IIB^{Man} are schematically displayed in Fig. 2. The six-stranded parallel β-sheet and the two-stranded antiparallel β-sheet are well defined by strong sequential $C^{\alpha}H_i/HN_{i+1}$ as well as long-range interstrand NOEs (see Fig. 3). Helix 4 (93–103), helix 5 (130–144) and helix 6 (158–164) are also well defined by strong $HN\text{-}HN_{(i+1)}$ NOEs and a large number of long-range connections ($C^{\alpha}H_i;HN_i/HN_{i+3};HN_{i+4}$). Helices 1 (27–31), 2 (48–55) and 3 (71–77) display strong $HN\text{-}HN_{(i+1)}$ NOEs but a lack of long-range connections, due to the low signal intensities around the phosphorylation site His^{20}.

Helices and strands were further confirmed by the CSI (Chemical Shift Index) method [25], evaluating the characteristic deviations of the C^{α}, C^{β}, CO and H^{α} chemical shifts from their random coil values. These secondary structure-dependent chemical shift deviations together with the CSI derived thereof (Fig. 4) are in excellent agreement with the secondary structure as determined from the NOE pattern. Especially the helices 1, 2 and 3 (where NOE data were scarce) could be confirmed by the characteristic CSI.

Finally, the $^{3}J_{HN,H\alpha}$ coupling constants were also found to be consistent with the IIB^{Man} secondary structure, with characteristic values for residues in α-helices (≈4 Hz) and β-sheets (≈9 Hz). Again, deuteration of the sample produced a considerable improvement of the HNHA spectrum (as already observed in the NOESY experiment, see above) with an dramatically increased number of HNHA cross-peaks. The different relaxation behavior of such a sample [26] can introduce additional errors in this method [20]; nevertheless the tendency of the measured coupling constants is in good agreement with the other indicators of secondary structure (see Fig. 2).

3.3. Biological implications

The IIB domain is an open twisted parallel β-sheet surrounded by helices on both sides. The underlying structure are two Rossmann folds (βαβαβ) which, like in a nucleotide-binding protein, are connected by an α-helix (Fig. 5). However, in contrast to the nucleotide-binding proteins, β-

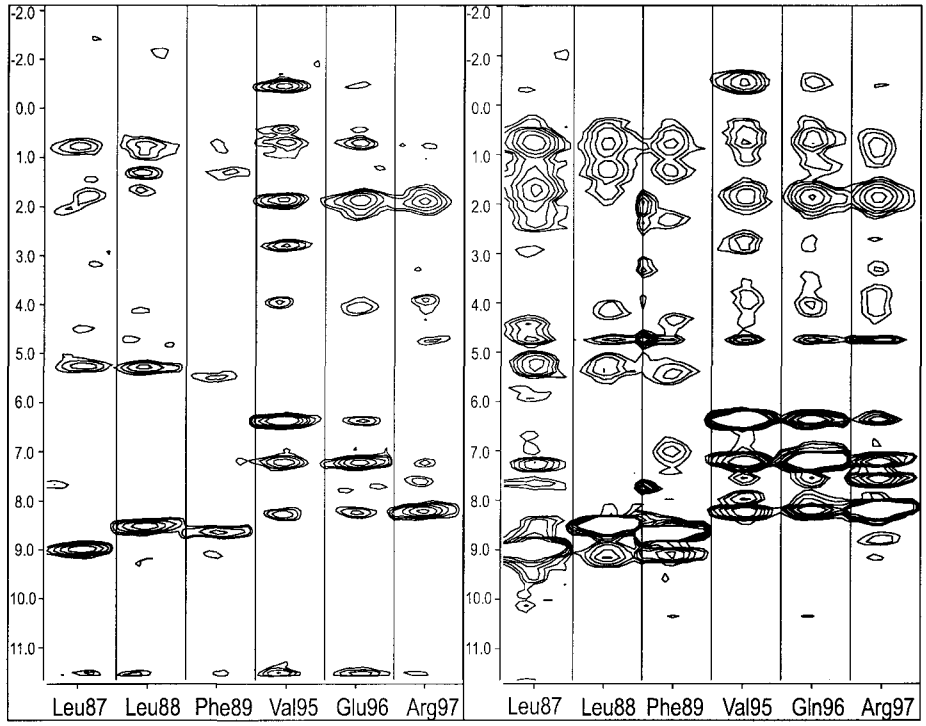

Fig. 1. Selected regions from the $^{1}H,^{1}H$-planes of a 3D ^{15}N-edited $^{1}H,^{1}H$-NOESY spectrum of IIB^{Man}. Slices were taken at the ^{15}N chemical shift of the indicated residues; residues 87–89 are located in a β-sheet, residues 95–97 in a helical region. Left panel: slices from the ^{15}N-labeled sample; right panel: slices from the uniformly 75% deuterated $^{15}N,^{13}C$-labeled sample. Under identical conditions the partially deuterated sample yields a significantly higher signal intensity and number of NOE correlations.

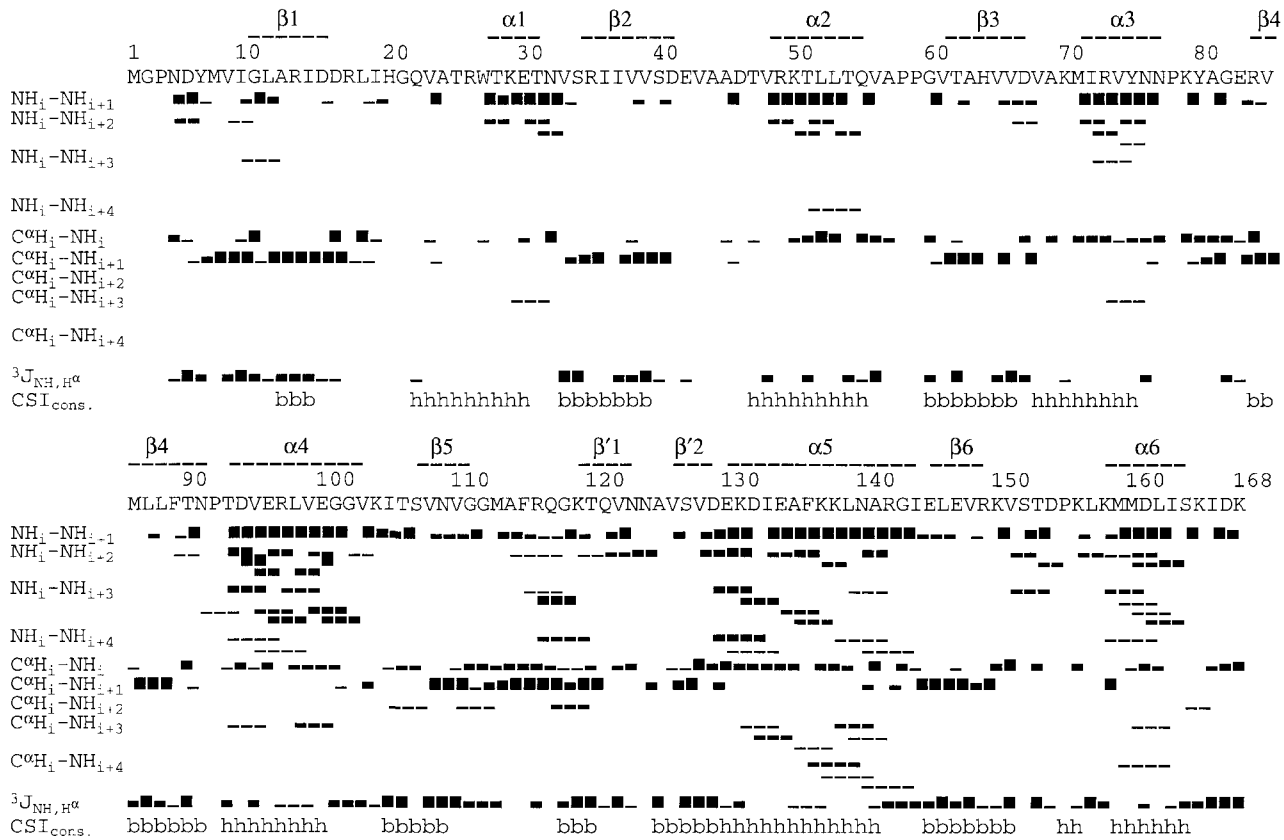

Fig. 2. Summary of sequential NOEs and $^{3}J_{HN,H\alpha}$ coupling constants. The width of the bars indicates the intensities of the corresponding NOEs (strong, strong-medium, medium, medium-weak, weak) and coupling constants (small, <2 Hz; medium, 2–5 Hz; large, >5 Hz). The secondary structure elements of IIB^{Man} are indicated on top.

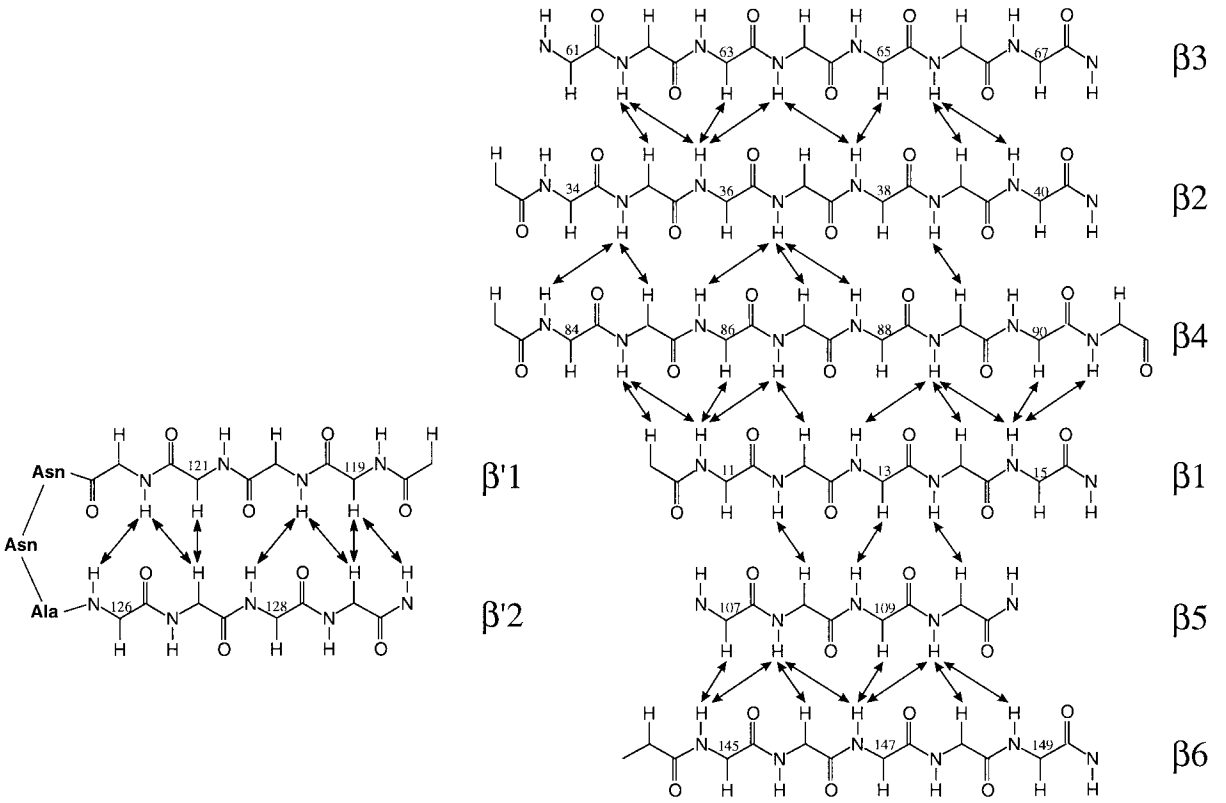

Fig. 3. Schematic representation of the central six-stranded parallel β-sheet and the two-stranded antiparallel β-sheet region. Arrows denote experimentally observed interstrand NOEs. All side chains have been omitted; the residue number is indicated at the α-carbon position.

strands 1 and 4 of IIB are swapped and the Rossmann folds are not adjacent (strands order 654123), but interdigitated (strand order 651423). Assuming that the alternating α and β structures form right-handed turns, then helices 1 and 2 are located on one side and helices 3, 4 and 5 on the opposite side of the β-sheet. The active site His^{20} is situated in the first loop (β1/α1) of the topological switch point. A comparison of IIB^{Man} with the three homologous proteins IIB^{Lev} (*B. subtilis* [27]), IIB^{Sor} (*K. pneumoniae* [28] and IIB^{Glc} (*V. furnissii*) (C. Bouma and S. Roseman, personal communication) indicates that the sequences at the active site are strongly conserved (**R**ID(D/E)**R**(L/F)(I/V)**H**GQV. The invariant arginines Arg^{13} and Arg^{17} are indispensable for phosphoryl transfer from His^{20} to the 6′-OH of mannose, but not for phopshorylation of IIB by IIA (Lanz and Erni, unpublished observation). The entire first half of the β-sheet (β1 to β4) and especially the residues around the active site region of IIB^{Man} yielded only weak signals in all NMR experiments, suggesting a high degree of conformational flexibility. A possible explanation for this feature is that IIB interacts with up to four other protein domains, namely the two subunits of the intertwined IIA dimer [29] from which it receives the phosphoryl group, and the transmembrane IIC/IID subunits to at least one of which it is tightly bound (Erni, unpublished results). The interaction with IIA does not appear to influence IIB stability, because subclonal IIB and the IIB in the intact $IIAB^{Man}$ dimer show the same stability against thermal and GuHCl induced unfolding [30]. The stabilities of subclonal IIB and IIB in the complex with IIC and IID have not yet been compared. However, a $IIAB^{Man}$ mutant with a strongly reduced affinity for IIC/IID was discovered when different histidine mutants were characterized [6]. The mutant H219Q (corresponding to His^{64} in subclonal IIB) resides in β3 in the section of the protein displaying increased mobility. We speculate that this region is part of the interface with IIC/IID and that the absence of the protein–protein contacts could be responsible for the increased flexibility here.

No proteins of similar fold could be found in the SCOP database [31]. While this work was in progress, the secondary structure of the IIB^{Lev} subunit of the *B. subtilis* fructose transporter was solved by heteronuclear NMR [8]. The amino acid sequences of the two proteins are 43% identical. As expected, the two proteins show an almost identical secondary structure pattern. There are a few differences however: the small antiparallel β-sheet (β′1/β′2) and α6 of IIB^{Man} have not been found in IIB^{Lev}. On the other hand, an additional β-strand (β7) antiparallel to β6 was detected in IIB^{Lev}. For IIB^{Man} two NOE contacts (E147/L157; V148/K156) were indeed found at the position homologous to the β7 of IIB^{Lev} (i.e., K156-M159 in IIB^{Man}), but no evidence for the existence of a β sheet could be detected from NOE patterns, CSI and J coupling constants.

Further experiments are in progress to study the structural changes induced by phosphorylation and interaction of IIB^{Man} with IIA^{Man}.

References

[1] Oschkinat, H., Müller, T. and Dieckmann, T. (1994) Angew. Chem. Int. Ed. Engl. 33, 277–293.
[2] Postma, P.W., Lengeler, J.W. and Jacobson, G.R. (1993) Microbiol. Rev. 57, 543–594.

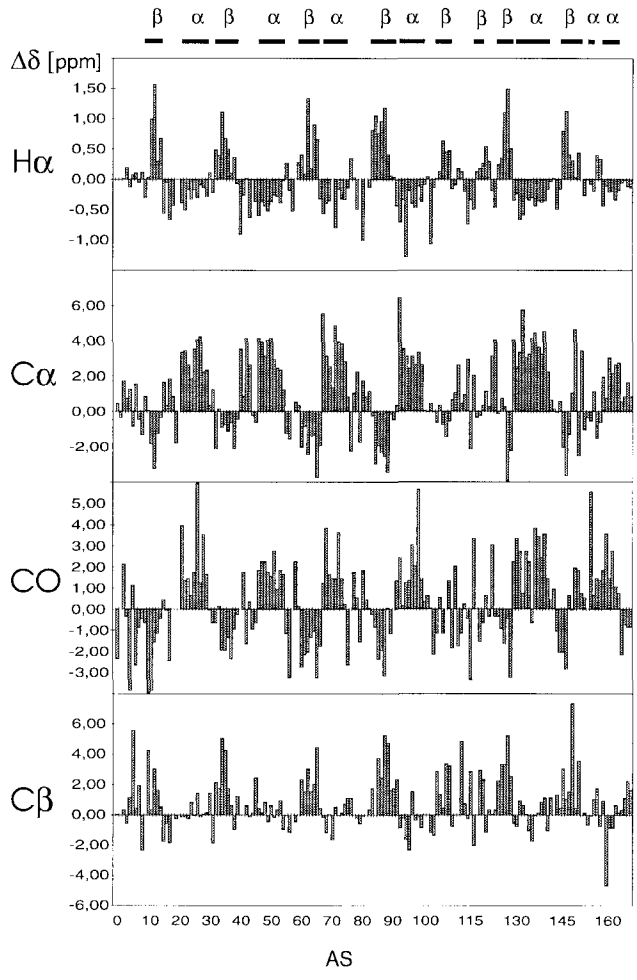

Fig. 4. Plot of the chemical shift deviations for each amino acid residue of IIB^{Man} from random coil shifts. Positive values correspond to a low-field shift relative to random coil. α-helices cause a positive deviation for C^{α} and CO and a negative deviation for the H^{α} and C^{β} resonances. In contrast, β-sheets are characterized by deviations in the opposite sense. The consensus secondary structure is indicated on the top.

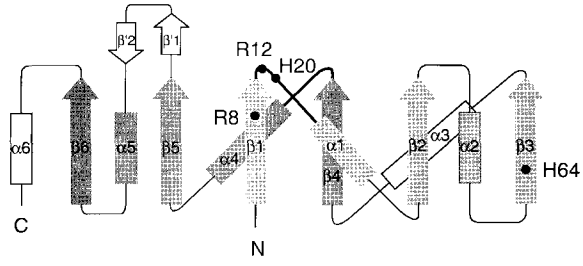

Fig. 5. Open twisted sheet topology of the IIB^{Man} domain. The two Rossmann folds are shown in different grey shades. The active site/phosphorylation site His^{20} is located at the topological switch point. The invariant residues Arg^{13} and Arg^{17} are essential for phosphoryl transfer from His^{20} to the hexose substrate.

[3] Saier, M.H., Jr., Chauvaux, S., Deutscher, J., Reizer, J. and Ye, J.-J. (1995) Trends Biochem. Sci. 20, 267–271.
[4] Erni, B., Zanolari, B. and Kocher, H.P. (1987) J. Biol. Chem. 262, 5238–5247.
[5] Mukhija, S. and Erni, B. (1996) J. Biol. Chem. 271, 14819–14824.
[6] Erni, B., Zanolari, B., Graff, P. and Kocher, H.P. (1989) J. Biol. Chem. 264, 18733–18741.
[7] Postma, P.W., Lengeler, J.W., and Jacobson, G.R. (1996) Phosphoenolpyruvate: carbohydrate phosphotransferase systems. in: *Escherichia coli* and *Salmonella*: cellular and molecular biology (Neidhardt, F.C. et al. eds.), pp. 1131–1149, ASM Press, Washington, DC.
[8] Seip, S., Lanz, R., Gutknecht, R., Flückiger, K. and Erni, B. (1996) Eur. J. Biochem. (in press).
[9] Wishart, D.S., Bigam, C.G., Yao, J., Abildgaard, F., Dyson, H.J., Oldfield, E., Markley, J.L. and Sykes, D. (1995) J. Biomol. NMR 6, 135–140.
[10] Palmer III, A.G., Cavanagh, J., Wright, P.E. and Rance, M. (1991) J. Magn. Reson. 93, 151–170.
[11] Kay, L.E., Keifer, P. and Saarinen, T. (1992) J. Am. Chem. Soc. 114, 10663–10665.
[12] Schleucher, J., Sattler, M. and Griesinger, C. (1993) Angew. Chem. 105, 1518–1521 and Angew. Chem., Int. Ed. Engl. 32, 1489–1491.
[13] Bax, A. and Pochapsky, S. (1992) J. Magn. Reson. 99, 638–643.
[14] Marion, D., Ikura, M., Tschudin, R. and Bax, A. (1989) J. Magn. Reson. 85, 393–399.
[15] Bax, A., Mehlkopf, A.F. and Smidt, J. (1979) J. Magn. Reson. 35 167–169.
[16] Powers, R., Gronenborn, A.M., Clore, G.M. and Bax, A. (1991) J. Magn. Reson. 94, 209–213.
[17] Jahnke, W. and Kessler, H. (1995) Angew. Chem. 107, 536–538 and Angew. Chem. Int. Ed. Engl. 34, 469–471.
[18] Yamazaki, T., Lee, W., Arrowsmith, C.H. Muhandiram, D.R. and Kay, L.E. (1994) J. Am. Chem. Soc. 116, 11655–11666.
[19] Shaka, A.J., Keeler, J., Frenkiel, T. and Freeman, R. (1988) J. Magn. Reson. 52, 335–338.
[20] Vuister, G.W. and Bax, A. (1993) J. Am. Chem. Soc. 115, 7772–7777.
[21] Shaka, A.J., Barker, P.B. and Freeman, R. (1985) J. Magn. Reson. 64, 547–552.
[22] Leutner, M., Gschwind, R.M. and Kessler, H. (1996) J. Biomol. NMR, submitted.
[23] Wüthrich, K. (1986) NMR of Proteins and Nucleic Acids, Wiley, New York.
[24] Nietlispach, D., Clowes, R.T., Broadhurst, R.W., Ito, Y., Keeler, J., Kelly, M., Ashurst, J., Oschkinat, H., Domaille, P.J. and Laue, E.D. (1996) J. Am. Chem. Soc. 118, 407–415.
[25] Wishart, D.S. and Sykes, B.D. (1994) J. Biomol. NMR 4, 171–180.
[26] Markus, M.A., Dayie, K.T., Matsudaira, P. and Wagner, G. (1994) J. Magn. Reson. B 105, 192–195.
[27] Martin-Verstraete, I., Dèbarbouillè, M., Klier, A. and Rapoport, G. (1990) J. Mol. Biol. 214, 657–671.
[28] Wehmeier, U.F. and Lengeler, J.W. (1995) Mol. Gen. Genet. 246, 610–618.
[29] Nunn, R.S., Markovic-Housley, Z., Gènovèsio-Taverne, J.C., Flükiger, K., Rizkallah, P.J., Jansonius, J.N., Schirmer, T. and Erni, B. (1996), J. Mol. Biol. 259, 502–511.
[30] Markovic Housley, Z., Cooper, A., Lustig, A., Flükiger, K., Stolz, B. and Erni, B. (1994) Biochemistry 33, 10977–10984.
[31] Murzin, A.G., Brenner, S.E., Hubbard, T. and Chotia, C. (1995) J. Mol. Biol. 247, 536–540; release 1.32, May 1996, http://scop.mrc-lmb.cam.ac.uk/scop.